

Electronic Supplementary Information

Taro leaf-inspired and superwetable nanonet-covered nanofibrous membranes for high-efficient oil purification

Jichao Zhang,^a Jianlong Ge,^a Yang Si,^{ab} Feng Zhang,^a Jianyong Yu,^{ab} Lifang Liu^a and
Bin Ding^{*ab}

*^aState Key Laboratory for Modification of Chemical Fibers and Polymer Materials,
College of Textiles, Donghua University, Shanghai 201620, China*

*^bInnovation Center for Textile Science and Technology, Donghua University, Shanghai
200051, China*

**E-mail: binding@dhu.edu.cn*

Experimental section

Materials

PVDF powder ($M_w = 570,000 \text{ g mol}^{-1}$) were obtained from Solvay Industries Ltd. Lithium chloride (LiCl) and span 80 were supplied by Sigma-Aldrich. N, N-dimethylformamide (DMF), petroleum ether, cyclohexane, isooctane, methanol, ethanol, and 1-propanol were all purchased from Aladdin. Diesel was supplied by Sinopec Shanghai Petrochemical Co., Ltd., China. Ultrapure water was obtained from Millipore system. The nonwoven substrate (polyethylene terephthalate) for the collection of fibers was provided by Tianjin Teda Filter Co., Ltd., China. Diesel was prefiltered by a UF membrane (Millipore SLFG05000, average pore size of $0.2 \mu\text{m}$) before use. All the other reagents were analytical grade and no more purified.

Construction of fibrous porous substrate

The precursor solution system for fabrication of the substrate in this work was prepared by dissolving 22 wt% PVDF powder and 0.02 wt% LiCl in DMF under continuous mechanical stirring for 10 h at 80°C . The electrospinning process was performed on a spinning machine (DXES, SOF Nanotechnology Co., Ltd, China). PVDF solution was loaded into syringes with 22-G metal nozzle with a controllable flow rate of 2 mL h^{-1} . A high voltage of 30 kV was applied to the nozzle tips, resulting in the deposition of PVDF fibers on the nonwoven substrate covered grounded stainless roller with a 22 cm tip-to-collector distance. The rotation speed of the roller was steadily kept at 50 rpm. The ambient temperature and relative humidity were controlled at $23 \pm 2^\circ\text{C}$ and $50 \pm 3\%$. In order to improve the uniformity of fibrous membrane, we placed plastic syringes

at equal spacing on the injection pump, which horizontally moved backwards and forwards at a constant speed within a fixed distance by using the mechanical slide unit. And, simple electric shield device on every needle was also employed to ensure that the jets were flying forward, thus the fibers could be uniformly deposited during the quadrature motion process caused by the synchronous movement of the stainless roller and mechanical slide unit.

Fabrication of biomimetic skin layer

The dilute solutions with PVDF concentrations of 1, 3, 6 and 9 wt% containing 0.1 wt% LiCl were prepared respectively. The skin layer was fabricated through the machine similar to above. The flow rate of the solutions was 1 mL h⁻¹. A voltage of 25 kV was employed to eject relevant solutions. The former prepared porous membrane was coated onto the grounded stainless roller and used as the collector. The tip-to-collector distance was fixed at 25 cm. The ambient temperature and relative humidity were kept at 23 ± 2 °C and 20 ± 2%, respectively. A series of dilute solutions with various PVDF concentrations were directly ejected on the substrate surface for a constant time of 9 h. To obtain the biomimetic composite membrane with the skin of different basis weight, the solution with 6 wt% PVDF was electrohydrodynamic ejected for 1, 5, 9, 11 h. All samples were dried in a vacuum oven at 75 °C for 2 h to eliminate residual solvent. The uniformity of biomimetic skin layer was controlled by the method similar to above.

Preparation of water-in-oil emulsions

For water-in-oil surfactant-free emulsions, water was mixed with oil (i.e. diesel, petroleum ether, isooctane, and cyclohexane) at a certain volume ratio (water/oil (v/v)

= 1/9) and then sonicated the mixtures for 1.5 h at a power of 560 W to produce milky emulsions. To prepare water-in-oil surfactant-stabilized emulsions, span 80 (0.2 mg mL⁻¹) was first dissolved in oil (i.e. diesel, petroleum ether, isooctane and cyclohexane), then a certain amount of water (water/oil (v/v) = 1/99) was added. The mixtures were sonicated under the same power for 1 h. All the surfactant-stabilized emulsions can stabilize for more than 20 days without obvious precipitation. The detail information about prepared emulsions was shown in Table S2.

Emulsion separation experiments

The evaluation of the emulsion separation performance of the membranes was conducted using a dead-end filtration apparatus equipped with a vacuum pump. The as-prepared membranes were sandwiched between glass reservoir and funnel base with a diameter of 20 mm. The freshly prepared emulsion was poured into separation cell and separated under gravity or vacuum pump pressure. The flux of membrane was determined by the equation as follows: $J = \frac{V}{At}$, where V is the oil volume, A is the effective area and t is the testing time, here it is 1 min. The heights of emulsions column were adjusted to afford a constant gravitational pressure of 1 kPa during the separation process with or without external driving pressure. In view of the densities of oils, the heights were approximate 12.2, 12.8, 14.5, and 15.2 cm for water-in-diesel, water-in-cyclohexane, water-in-isooctane, and water-in-petroleum emulsions, respectively. The external pressure was controlled by a pump equipped with a tee valve.¹ The water contents in the collected filtrates were analyzed by Karl Fischer titrator. For every emulsion, at least three times were tested to acquire an average value.

Characterization

The precursor solutions properties (viscosity, conductivity and surface tension) were measured using a viscometer (DV3TLV, Brookfield, America), a conductivity meter (Seven2Go, Mettler-Toledo, Switzerland), and a surface tension meter (K100, Krüss, Germany), respectively. The morphologies of the membranes were characterized using a scanning electron microscopy (SEM) (S-4800, Hitachi, Japan). The arithmetic average roughness (Ra) of the membranes was determined on a non-contact optical profilometer (ContourGT-K, Bruker, America). The surface topography and Ra of microsphere were detected by an atomic force microscopy (MFP-3D, Asylum Research, America). The mechanical property was measured using a tensile instrument (XQ-1C, Lipu, China). The porous structure of membranes was characterized using a capillary flow porometer (PoroLux 1000, Porometer, Germany) and the water intrusion pressure measurement was carried out using the same machine. For testing the pore size, the membrane was thoroughly infiltrated by wetting liquid (Porefil, surface tension 16 dyn cm^{-1}). The liquid was constrained in the pores as a result of the liquid surface tension. An increasing air pressure was exerted on the membrane, and when the air pressure was larger than the liquid surface tension, the liquid trapped in the pores was extruded. The liquid in the largest pores was crowded out firstly, and then with increasing pressure the gas would flow through the small pores and finally all the pores were emptied. The average flow pore size and pore size distribution were calculated according to the relationship between airflow rate and air pressure for the wet sample and the dry sample.

Three specimens from each membrane were tested to ensure the repeatability and representativeness of the obtained porous structure data.²⁻⁴ For testing under-oil intrusion pressure, the membrane was firstly completely wetted by related oil and covered with pure water after being placed in the sealed chamber. Water contact angle (3 μL), oil contact angle (3 μL), under-oil water contact angle (3 μL), and sliding angle (10 μL) were performed on a contact angle goniometer (SL 200B, Kino, America). The adhesion force were tested by a high-sensitivity microelectromechanical balance system (DCAT 11, Data Physics, Germany). The size of water droplet in emulsions was measured by dynamic light scattering (BI-200SM, Brookhaven, America). Optical microscopy images were recorded on a microscope (VHS-3000, Olympus, Japan). The water content in oil was detected by a Karl Fischer titrator (831KF Coulometer, Metrohm, Switzerland).

Supplementary Materials

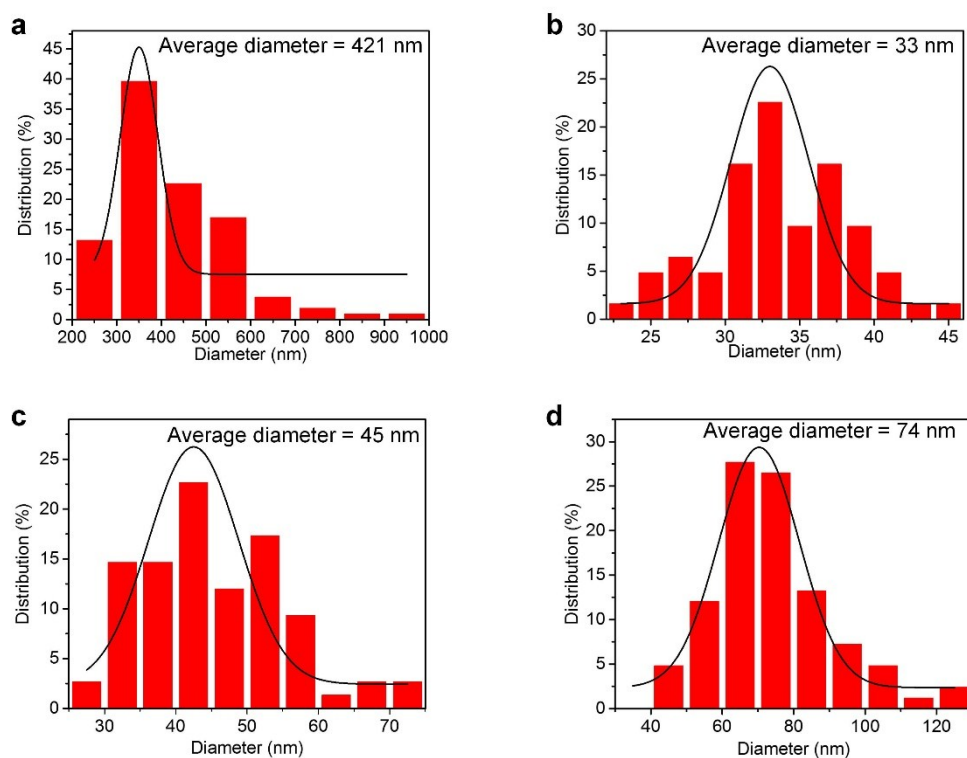


Fig. S1 (a) Histogram showing the fiber diameter distribution of the 22 wt% PVDF electrospun fibrous membrane (EFM). Histogram showing the nanowire diameter distribution in 3 wt% (b), 6 wt% (c), 9 wt% (d) PVDF skin layer.

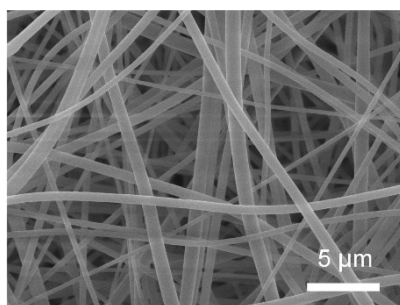


Fig. S2 SEM image of the pristine 22 wt% PVDF EFM.

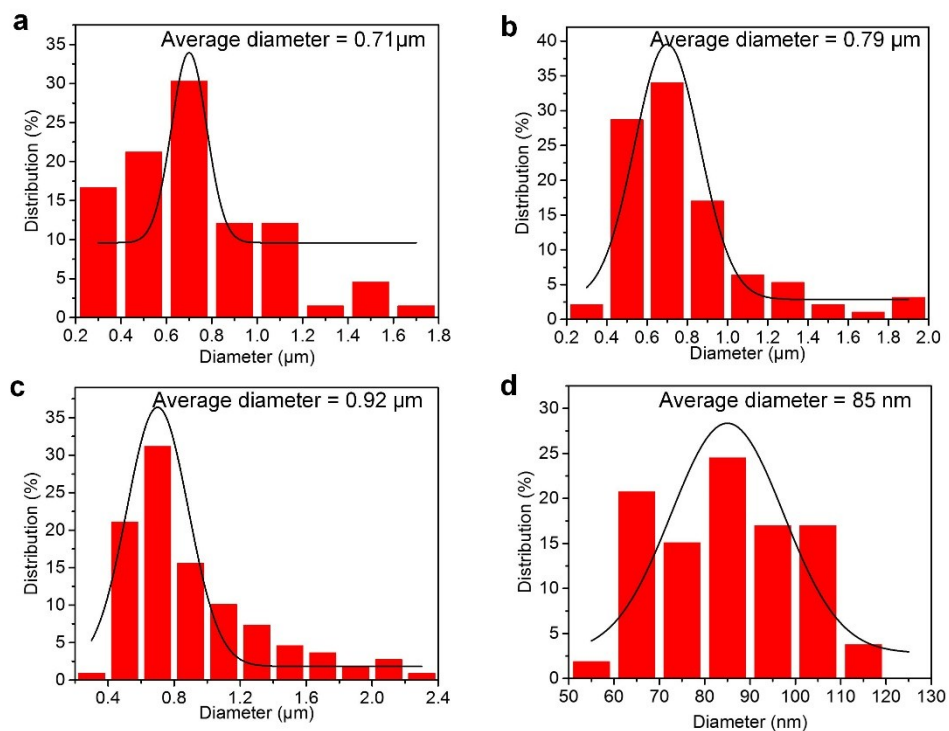


Fig. S3 Histogram showing the microsphere diameter distribution of 1 wt% PVDF skin layer (d), 3 wt% PVDF skin layer (b), and 6 wt% PVDF skin layer (c). Histogram showing the nanobead diameter distribution of 6 wt% PVDF skin layer.

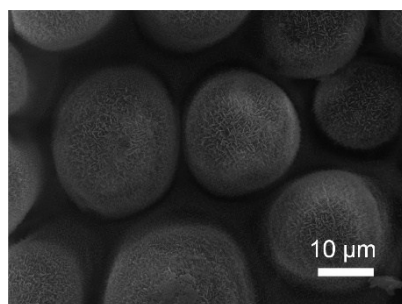


Fig. S4 SEM image of a taro leaf consisting of several micrometers spheres at low magnification.

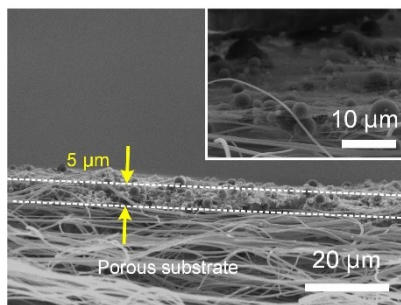


Fig. S5 Enlarged SEM images of the composite membrane with 6 wt% PVDF skin layer.

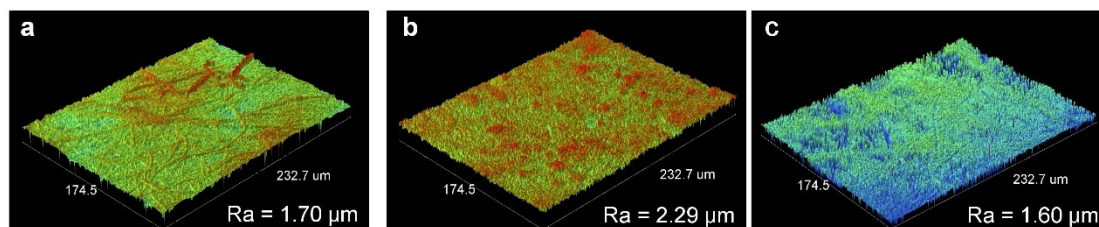


Fig. S6 The three-dimensional optical profilometry images of composite membranes with 1 wt% (a), 3 wt% (b), and 9 wt% (c) PVDF skin layer.

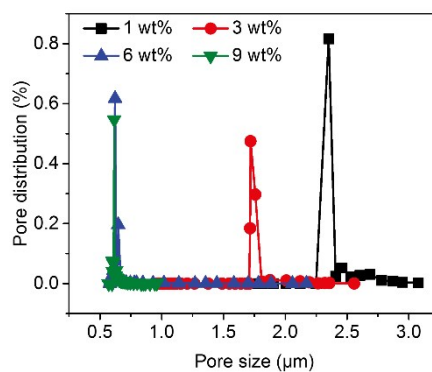


Fig. S7 Pore size distribution of the composite membranes with 1, 3, 6, and 9 wt% PVDF skin layer.

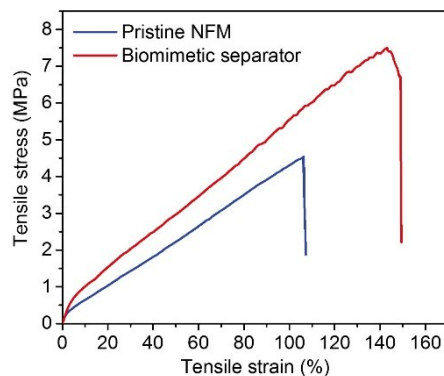


Fig. S8 Stress-strain curve of pristine 22 wt% PVDF EFM and the composite membrane with 6 wt% PVDF skin layer.

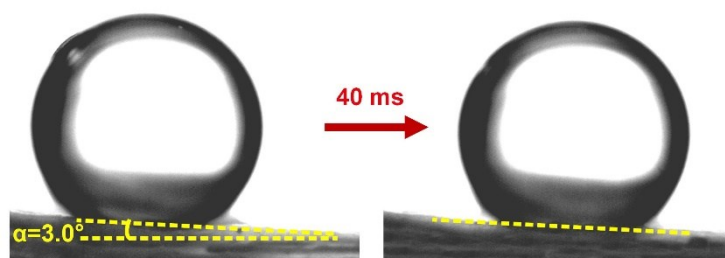


Fig. S9 Photograph of a water droplet sliding on the biomimetic membrane under diesel.

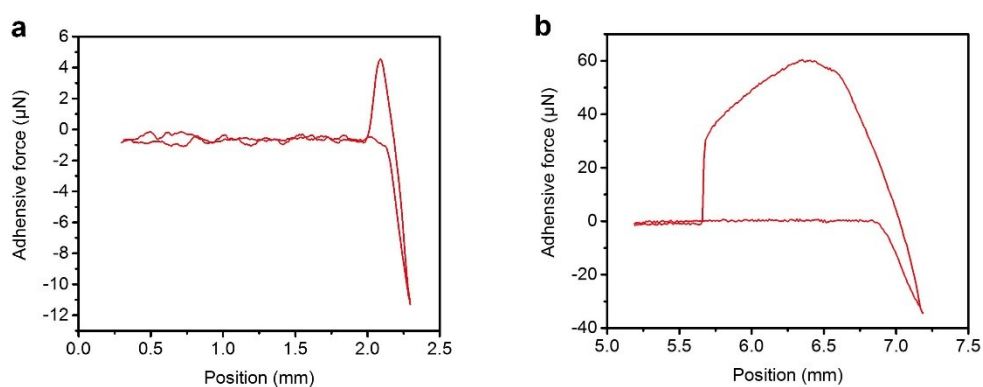


Fig. S10 Real-time recorded force-distance curves during the dynamic water adhesion measurements on biomimetic membrane (a) and pristine EFM (b).

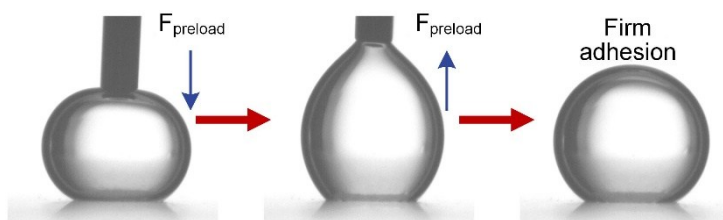


Fig. S11 Photographs of a water droplet forced to contact and lift from the 6 wt% PVDF flat membrane under-oil.

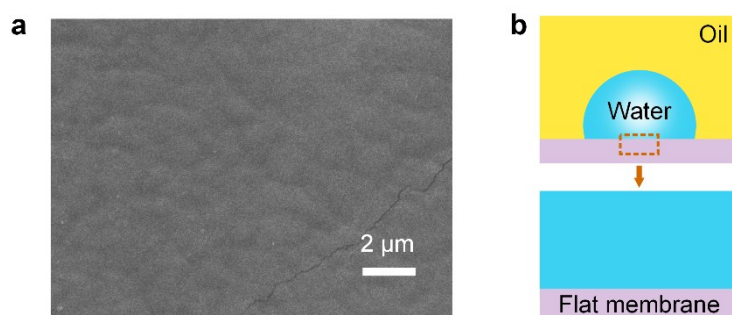


Fig. S12 (a) SEM image of the 6 wt% PVDF flat film. (b) Schematic showing flat membrane in Wenzel state.

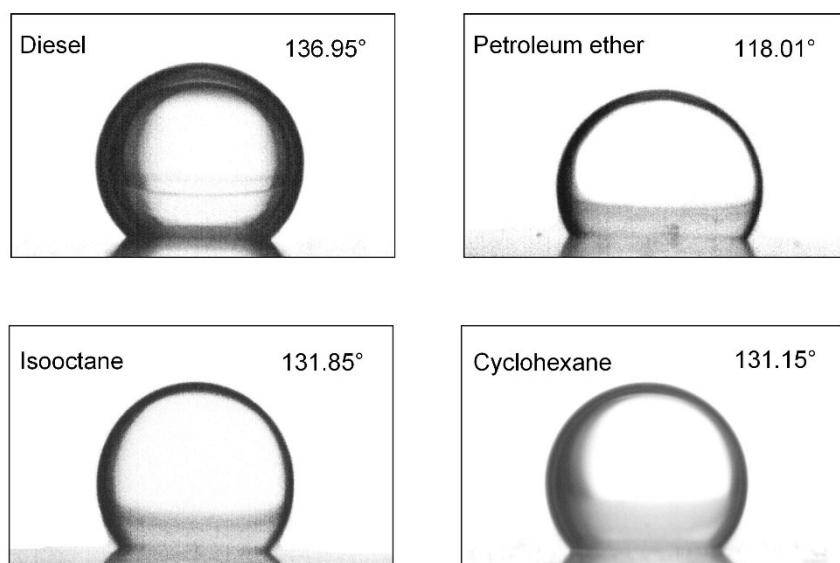


Fig. S13 Digital photos of water droplets on the surface of the 6 wt% PVDF flat membrane under various oils.

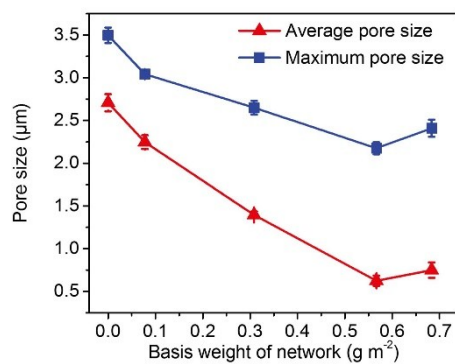


Fig. S14 Maximum and average pore size of biomimetic membranes with various basis weight of 6 wt% PVDF layer.

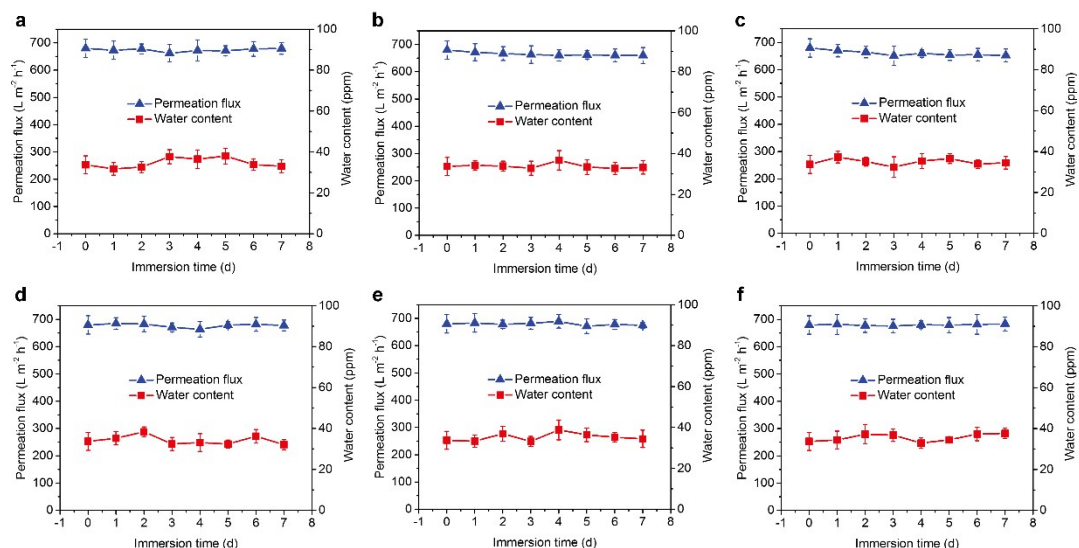


Fig. S15 Permeation fluxes and water contents in filtrates of our PVDF biomimetic membranes for water-in-petroleum ether SFE separation versus immersion time in (a) petroleum ether, (b) isooctane, (c) cyclohexane, (d) methanol, (e) ethanol, and (f) 1-propanol.

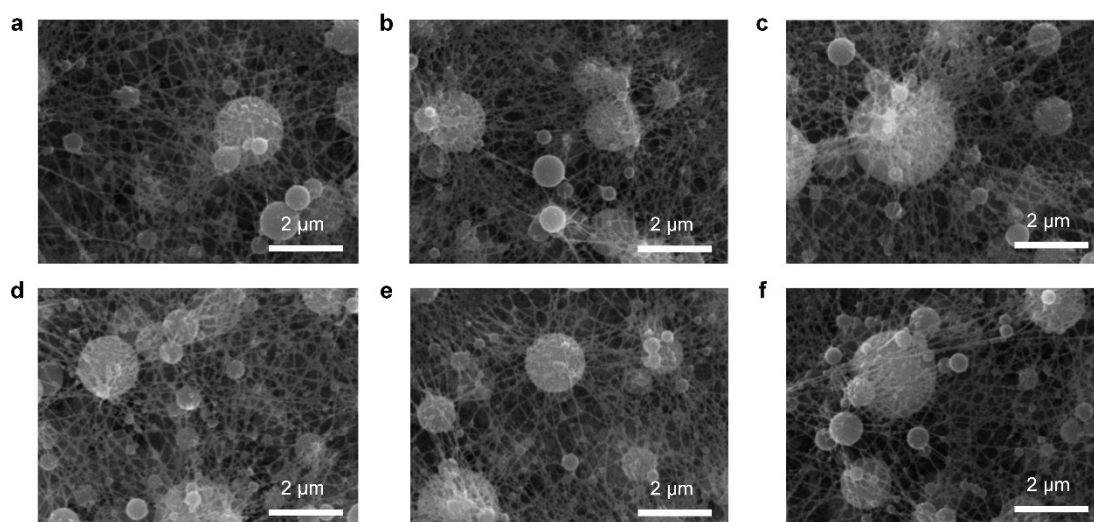


Fig. S16 Morphology of PVDF biomimetic membranes after immersion in different organic solvent for one week: (a) petroleum ether, (b) isooctane, (c) cyclohexane, (d) methanol, (e) ethanol, and (f) 1-propanol.

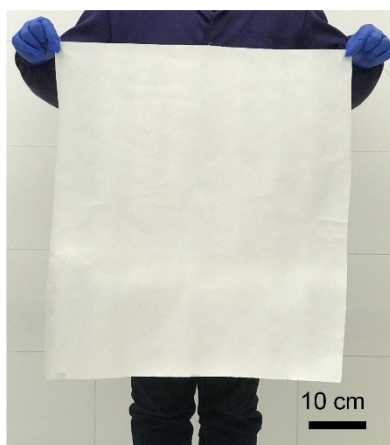


Fig. S17 Photograph of a large-scale ($50 \times 60 \text{ cm}^2$) biomimetic membrane with 6 wt% PVDF skin layer.

Table S1. Summary of the properties of the precursor solutions with different concentrations of PVDF.

Concentration (wt %)	Viscosity (mPa·s)	Surface tension (mN m ⁻¹)
1	7	35.34
3	16	35.63
6	35	35.45
9	316	34.73
22	938	34.89

Table S2. Summary of the properties of the oils and the water content of related emulsions.

Oils	Viscosity (mPa·s)	Density (g cm ⁻³)	Surface tension (mN m ⁻¹)	Water content of SFE (ppm)	Water content of SSE (ppm)
Petroleum ether	0.30	0.66	18.83	347	5387
Isooctane	0.53	0.69	22.60	809	7924
Cyclohexane	1.00	0.78	24.33	2317	7429
Diesel	3.50	0.82	28.37	8596	5966

Supplementary Methods

The details about the study of intrusion pressure

As for water intrusion pressure in air, $P = -\frac{4\gamma \cos \theta_{adv}}{d_{max}}$, where d_{max} is the maximum pore size of the membrane, γ is water surface tension, and θ_{adv} is the advancing water contact angle of PVDF flat membrane in air, which represents wettability at pores surface and avoids the influence of roughness derived from fibrous structure.⁵

As for under-oil water intrusion pressure, the equation is $P = -\frac{4\gamma_{ow} \cos \theta_{adv}}{d_{max}}$, where γ_{ow} is the water/oil interfacial tension, θ_{adv} is the under-oil advancing oil contact angle on PVDF flat membrane surface and d_{max} is the maximum pore size of the membrane.⁶ The water/oil interfacial tensions of various oils were measured on a surface tension meter (K100, Krüss, Germany) at ambient temperature. The experimental intrusion pressure values were achieved by a capillary flow porometer (PoroLux 1000, Porometer, Germany). Here we take diesel and cyclohexane as examples. The interfacial between oil with surfactant (0.2 mg ml⁻¹) and water was 22.43 mN m⁻¹ and 25.09 mN m⁻¹, respectively.

The details about the study of water droplets collision in oil

In the experiments, a custom-built cell was filled with oil, and a dyed water droplet was firstly placed on the bottom of the cell. Subsequently, another water droplet dripped from the top and came into contact with the lower droplet.

Movie S1: The coalescence of water droplets after colliding in cyclohexane.

Movie S2: The detachment of water droplets after colliding in cyclohexane with surfactants (span 80: 0.2 mg mL⁻¹).

Movie S3: The coalescence of water droplets after colliding in diesel.

Movie S4: The detachment of water droplets after colliding in diesel with surfactants (span 80: 0.2 mg mL⁻¹).

Movie S5: The membrane module can enable continuous collection of oil from water-in-diesel SSE.

References

1. J. Ge, D. Zong, Q. Jin, J. Yu and B. Ding, *Adv. Funct. Mater.*, 2018, 1705051.
2. K.-K. Yan, L. Jiao, S. Lin, X. Ji, Y. Lu and L. Zhang, *Desalination*, 2018, 437, 26-33.
3. R. Zheng, Y. Chen, J. Wang, J. Song, X.-M. Li and T. He, *J. Membr. Sci.*, 2018, 555, 197-205.
4. Z. Zhu, Z. Liu, L. Zhong, C. Song, W. Shi, F. Cui and W. Wang, *J. Membr. Sci.*, 2018, 563, 602-609.
5. Y. Li, F. Yang, J. Yu and B. Ding, *Adv. Mater. Interfaces*, 2016, **3**, 1600516.
6. Z. Xue, S. Wang, L. Lin, L. Chen, M. Liu, L. Feng and L. Jiang, *Adv. Mater.*, 2011, **23**, 4270-4273.